LAWRENCE
LIVERMORE
NATIONAL
LABORATORY

UCRL-JRNL-202263

Coral Radiocarbon Records of Indian Ocean Water Mass Mixing and Wind-Induced Upwelling Along the Coast of Sumatra, Indonesia

N. S. Grumet, N. J. Abram, J. W. Beck, R. B. Dunbar, M. K. Gagan, T. P. Guilderson, W. S. Hantoro, B. W. Suwargadi

February 9, 2004

Journal of Geophysical Research

Coral radiocarbon records of Indian Ocean water mass mixing and wind-induced upwelling along the coast of Sumatra, Indonesia

N.S. Grumet[1], N.J. Abram[2], J.W. Beck[3], R.B. Dunbar[1], M.K. Gagan[2], T.P. Guilderson[4,5], W.S. Hantoro[6], and B.W. Suwargadi[6]

[1]Department of Geological and Environmental Sciences, Stanford University, Stanford, California 94305
[2]Research School of Earth Sciences, The Australian National University, Canberra, ACT 0200, Australia
[3]NSF AMS Facility, Department of Physics, University of Arizona, Tucson, Arizona, 85721
[4]Center for Accelerator Mass Spectrometry, Lawrence Livermore National Laboratory, Livermore, California 94551
[5]Institute of Marine Sciences, University of California at Santa Cruz, Santa Cruz, CA 65064
[6]Research and Development Center for Geotechnology, Indonesian Institute of Science (LIPI), Bandung 40135, Indonesia.

Abstract

Radiocarbon (^{14}C) in the skeletal aragonite of annually banded corals track radiocarbon concentrations in dissolved inorganic carbon (DIC) in surface seawater. As a result of nuclear weapons testing in the 1950s, oceanic uptake of excess ^{14}C in the atmosphere has increased the contrast between surface and deep ocean ^{14}C concentrations. We present accelerator mass spectrometric (AMS) measurements of radiocarbon isotope ($\Delta^{14}C$) in *Porites* corals from the Mentawai Islands, Sumatra (0ºS, 98ºE) and Watamu, Kenya (3ºS, 39ºE) to document the temporal and spatial evolution of the ^{14}C gradient in the tropical Indian Ocean. The rise in $\Delta^{14}C$ in the Sumatra coral, in response to the maximum in nuclear weapons testing, is delayed by 2-3 years relative to the rise in coral $\Delta^{14}C$ from the coast of Kenya. Kenya coral $\Delta^{14}C$ values rise quickly because surface waters are in prolonged contact with the atmosphere. In contrast, wind-induced upwelling and rapid mixing along the coast of Sumatra entrains ^{14}C-depleted water from the subsurface, which dilutes the effect of the uptake of bomb-laden ^{14}C by the surface-ocean. Bimonthly AMS $\Delta^{14}C$ measurements on the Mentawai coral reveal mainly interannual variability with minor seasonal variability. The interannual signal may be a response to

changes in the Walker circulation, the development of easterly wind anomalies, shoaling of the eastern thermocline, and upwelling of ^{14}C-depleted water along the coast of Sumatra. Singular spectrum analysis of the Sumatra coral $\Delta^{14}C$ record reveals a significant 3-year periodicity. The results lend support to the concept that ocean-atmosphere interactions between the Pacific and Indian Oceans operate in concert with the El Niño-Southern Oscillation (ENSO).

Introduction

The possibility that the Indian Ocean possesses an internal mode of climate variability independent from the Pacific Ocean has important implications for the predictability of climate in countries influenced by the Asian and Indian Monsoons. There is still considerable debate about the driving mechanisms for anomalous ocean-atmosphere conditions in the Indian Ocean (Saji et al., 1999; Webster et al., 1999; Allan et al., 2001; Hastenrath et al., 2002). Changes in the equatorial zonal winds appear to have a profound impact on equatorial ocean circulation, sea surface temperature (SST) and climate in the Indian Ocean region, as illustrated during unusual ocean-atmosphere conditions in 1994 (Behera et al., 1999; Vinayachandran et al., 1999) and 1997-1998 (Yu and Rienecker, 1999; Webster et al., 1999). Wind-induced upwelling along the coast of Sumatra for example, as well as interocean throughflow within the Indonesian Seas, play a critical role in determining SST patterns in the eastern Indian Ocean (Yu and Rienecker, 2000; Susanto et al., 2001). Significant interannual variability in upwelling in the eastern Indian Ocean has been linked to ENSO as well as ENSO-independent events (Feng et al., 2001; Huang and Kinter, 2002; Rao et al., 2002; Yu et al., 2002).

Improved understanding of unusual coupled ocean-atmosphere events, and their exact relationship with ENSO and global climate, requires the acquisition of high-quality proxy climate reconstructions, such as those provided by coral stable isotope and radiocarbon (^{14}C) records. In this paper we investigate the timing and amplitude of nuclear bomb produced ^{14}C as a tracer of air-sea exchange processes, mixing of bomb $^{14}CO_2$ between the surface mixed layer and upper ocean, and regional circulation off the coasts of Kenya and southwestern Indonesia (Fig. 1a). An intrabasin comparison of decadal-scale changes in surface ocean ^{14}C concentrations is made to better understand differences in water mass mixing in the equatorial Indian Ocean. We then explore the seasonal and interannual variability in coral ^{14}C from southwest Sumatra to understand the ocean-atmosphere processes driving climate variability in the eastern equatorial Indian Ocean.

Background

Radiocarbon as a Tracer for Water Mass Circulation

The analysis of transient anthropogenic tracers in the world's oceans, such as radiocarbon, has greatly enhanced our understanding of deep thermohaline circulation and ventilation of subthermocline waters (e.g., Rhein et al., 1995; Jenkins and Smethie, 1996). The deep ocean is depleted in ^{14}C relative to the surface ocean because of the long residence time of deep ocean water, which allows for significant ^{14}C decay ($t_{1/2}$ = 5730 yr). In contrast, the surface ocean is enriched in ^{14}C as a result of air-sea gas exchange and the slow replenishment of the surface waters with those from below. This surface water enrichment due to nuclear weapons testing in the 1950s makes the distribution of ^{14}C very sensitive to vertical mixing and a useful tracer of ocean circulation.

Surface and subsurface measurements of $^{14}C/^{12}C$ ($\Delta^{14}C$), such as those collected by the Geochemical Ocean Sections Study (GEOSECS), Indien Gaz Ocean (INDIGO), and World Ocean Circulation Experiment (WOCE) programs have improved our understanding of the intense monsoon driven upwelling that occurs off the coasts of Somalia and Arabia (e.g., Broecker et al., 1985; Bard et al., 1988; Ostlund and Grall, 1991). While results from these programs have been extremely valuable, vertical profiles are subject to temporal aliasing since the measurements represent a "snapshot" of ambient oceanic conditions. Such snapshots may be augmented with time-series such as those developed from biogenic archives.

Corals incorporate dissolved inorganic carbon (DIC) from the surrounding seawater into their skeletons. Measurements of $\Delta^{14}C$ in the skeletal aragonite of banded corals have been shown to provide an unaltered record of the $^{14}C/^{12}C$ ratio of DIC in ambient surface seawater (Druffel and Linick, 1978; Druffel, 1982; Druffel, 1989; Brown et al., 1993; Guilderson et al., 1998). Therefore, seawater ^{14}C concentrations can be determined for the past 100 years or more in many regions of the tropics and sub-tropics where corals grow. In addition, SST records reconstructed from oxygen isotope ratios ($\delta^{18}O$) can be correlated to coral $\Delta^{14}C$ to estimate the relative influence of ocean-atmospheric exchange and surface-ocean circulation processes on determining the ^{14}C content of equatorial waters (Druffel, 1987). For example, surface ^{14}C variability in the equatorial eastern Pacific near Galapagos is influenced by the vigor of upwelling and by the origin of upwelled water (Guilderson and Schrag, 1998). Such records provide boundary constraints used to test the parameterization of ocean dynamics in circulation

models such as changes in lateral and vertical water mass mixing (e.g., Rodgers et al., 1997; 2000).

Physical Oceanography

Circulation in the tropical Indian Ocean is a complex interplay between remote forcing from both the equatorial Indian and Pacific Oceans and the seasonally reversing African and Asian-Australian monsoons (e.g., Godfrey, 1996; Tourre and White, 1997; Potemra and Lukas, 1999). In particular, the Indian Ocean equatorial current system is dominated by a semi-annual flow reversal in a narrow band along the equator. As a result, thermocline depth and sea-level also vary semi-annually. For example, during the boreal summer when the flow is westward, the 20^{o}C isotherm shoals off the coast of Sumatra and deepens off the coast of Africa (Tomczak and Godfrey, 2003).

During the monsoon transition (May and November), the South Java Current (SJC) flows south-eastward under the influence of equatorial Kelvin waves forced by westerly wind bursts formed during the monsoon transition (Quadfasel and Creswell, 1992; Sprintall et al., 1999; 2000). In addition, sea-level rises along the coasts of Sumatra and Java in response to northward and southward propagating coastally trapped Kelvin waves (Clarke and Liu, 1994; Sprintall et al., 2000). In contrast, during the southeast monsoon (May-October) the SJC forms a strong westward current along the coast of Java, especially in August. Easterlies develop and intensify upwelling and shoaling of the thermocline (Schott et al., 2002). As a result of the upwelling, the shallow freshwater cap in this region disappears and eliminates the barrier layer, which helps facilitate diapycnal mixing (Quadfasel and Creswell, 1992; Sprintall et al., 1999).

The influence of the monsoons on reversals of surface circulation is also seen in the western equatorial Indian Ocean. The Somali Current (SC), recognized as the western boundary current that causes structural readjustment in the baroclinicity down to 1000 m (Tomczak and Godfrey, 2002), is responsible for strong upwelling during the Southwest (SW) Monsoon along the northern coasts of Somalia and Oman where surface waters are anomalously depleted in ^{14}C. During the Northeast (NE) monsoon, the wintertime SC flows equatorward towards the coast of Kenya. Thus, the SC acts to transport upwelled water across the equator during the NE Monsoon. As a result, the Kenya coral $\Delta^{14}C$ time-series is sensitive to western boundary upwelling by means of meridional transport within the SC (Grumet et al., 2002b). Coral $\Delta^{14}C$ records from the coasts of Sumatra and Kenya therefore provide ideal locations to monitor the sensitivity of surface water $\Delta^{14}C$ to changes in vertical and lateral mixing in the equatorial Indian Ocean.

Methods

An underwater hydraulic drill-rig was used to extract a 2.7 m-long core (PG2) from a massive colony of *Porites* coral from the Mentawai Islands in June 2001. The collection site is approximately 400 m offshore of Penang Island (0º08'S, 98º31'E), a small coral cay in the northern section of the Mentawai Island chain (Fig. 1b.). The coral colony was located in ~6 m water depth (~3 m to top of coral) on a sandy fore-reef slope that was exposed to open ocean conditions. A 63 cm coral core was collected from massive hermatypic corals *Porites lutea* from Watamu, Kenya in August 1996 for $\Delta^{14}C$ analysis (Grumet et al., 2002a,b). The Kenya coral site is approximately 600 m offshore

and 200 m landward of an intermittent barrier system. Water depth is about 7 m at the Watamu site.

The Mentawai coral core was slabbed parallel to the major growth axis and x-rayed to reveal the coral density banding. Petrographic analysis of thin sections from the core showed the original coral aragonite to be well preserved. Transects to be analyzed for stable isotopes ($\delta^{18}O$, $\delta^{13}C$) were first reduced to 2.5 mm thickness, then ultrasonically cleaned in milli-Q H_2O and dried at 40°C, following the method of Gagan et al. (1994). High-resolution samples were then precisely shaved at 0.4 mm to 0.5 mm increments (fortnightly to weekly resolution) along a continuous strip 2.5 mm thick by 2.5 mm wide using an automated milling system. Measurements of $\delta^{18}O$ and $\delta^{13}C$ were made at the Australian National University (Abram et al., in prep).

It is important to point-out that the Mentawai Island reefs experienced severe coral mortality during a giant red tide associated with strong upwelling in 1997 (Abram et al, in press). The coral $\delta^{18}O$ record shows that the coral core collected in June 2001 from a massive dead *Porites* colony had already bioeroded back to July 1992. This observation is based on the match between the high-resolution coral $\delta^{18}O$, which in this location primarily reflects SST with a secondary influence from precipitation/evaporation changes, with the IGOSS SST record that extends back to 1982. Counting of annual density band couplets and annual cycles of coral $\delta^{18}O$ forward in time from a distinctive cooling signal in 1961, an anomalously cold year in the instrumental SST record (Yamagata et al., 2002), also confirms this result.

The Mentawai chronology was developed from the coral $\delta^{18}O$ record to act as a "template" to guide the sampling frequency for the AMS measurements of coral $\Delta^{14}C$.

Annual "anchor points" were assigned to the annual $\delta^{18}O$ maximum, which falls in early December, the coolest time of year in the Mentawai region. The chronology was then linearly interpolated between these yearly markers. The $\delta^{13}C$ measurements from the stable isotope and $\Delta^{14}C$ samples were used to precisely match the adjacent $\Delta^{14}C$ transect with the chronology developed for the stable isotope transect.

Well-developed annual density bands and minimum and maximum $\delta^{18}O$ values were used to define the Watamu chronology (Grumet et al., 2000). Instrumental SST records indicate that the maximum (minimum) temperature off the coast of Kenya occurs in March/April (July/August). Accordingly, the minimum and maximum Watamu coral $\delta^{18}O$ values were assigned the corresponding calendar date. Samples in between these points were linearly interpolated in order to construct a sub-annually resolved age model. The assigned calendar months also show a strong correspondence to changes in density. The minimum $\delta^{18}O$ values in April coincide with high-density bands. As indicated by instrumental records, this is the warmest time of the year, when calcification exceeds extension (linear growth), resulting in the formation of high-density bands (Highsmith, 1979).

Samples for Mentawai AMS determinations of $^{14}C/^{12}C$ were collected adjacent to the stable isotope sampling transect using a low speed cutting tool to extract sample blocks between 1 mm and 1.5 mm resolution. At an apparent linear extension rate of 13 mm/yr and a maximum sample interval of 2.5 mm (every second sample), approximately 5 samples/yr were analyzed for $\Delta^{14}C$ between 1944 and 1990, yielding a ~bimonthly $\Delta^{14}C$ time-series. Radiocarbon samples between 1876 and 1880 were also analyzed to further characterize the pre-bomb period. Samples were prepared and analyzed at the

University of Arizona NSF Accelerator Mass Spectrometer Facility. Aragonite splits (~10 mg) were heated and acidified with orthophosphoric acid at 90ºC in individual reaction chambers. The evolved CO_2 was converted to graphite by catalytic reduction of CO_2 in the presence of zinc (Jull et al., 1986; Slota et al., 1987).

Radiocarbon results are reported as $\Delta^{14}C$ in per mil (‰), as defined by Stuiver and Polach (1977):

$$\Delta^{14}C = [[F_{modern} * e^{(\lambda * t)} - 1] * 1000]$$

where F_{modern} (Fraction Modern) is the measured $^{14}C/^{13}C$ ratio in the sample, normalized to $\delta^{13}C$=-25‰ divided by the calculated modern standard $^{14}C/^{13}C$ ratio (1950 AD), as determined from measurements of the NBS oxalic acid standard, also normalized to $\delta^{13}C$=-25‰, the decay coefficient $\lambda = {}^{1}/_{8267}$ yr^{-1} based on the 5730 yr half life, and t = 1950-calculated age (Linick et al., 1986; Donahue et al., 1990). These results are $\Delta^{13}C$ and age corrected to account for ^{13}C isotopic fractionation and decay between 1950 and calculated age. An external error of approximately ±6‰ is estimated for 285 modern-day coral $\Delta^{14}C$ analyses. The external error reflects the counting statistics on an individual measurement combined quadratically to the machine error (~2 to 3‰), which is calculated from the standard deviation of the oxalic acid standards (OX1 and OX11) over the course of 6 months. Watamu AMS determinations of $^{14}C/^{12}C$ are reported in Grumet et al. (2002a,b).

Results

Pre-bomb Period

The period from 1876-1880 in the PG2 core yields a pre-bomb average of -63‰ with a standard error of ±1‰ (n=25). This is in close agreement with a pre-bomb average

calculated from 1944-1954 of -65‰ with standard error of ±0.74‰ (n=66) (Fig. 2). Together these segments yield a pre-bomb average of -64‰ and a standard error of ~1‰. The decrease in pre-bomb average from 1877 to 1954 is less than 2‰. Pre-bomb Mentawai $\Delta^{14}C$ values range between –79‰ in the early boreal summer of 1949 to a maximum value of –52‰ in 1879 and –55‰ in 1944, 1946, and 1948. Except for the positive excursion in 1877, an historically cold year, there is no clear phase relationship between $\Delta^{14}C$ and $\delta^{18}O$ (Fig. 2).

Long Term Trend

Mentawai coral $\Delta^{14}C$ levels begin to respond to atmospheric testing in the mid 1950s and peak (~120‰) in the early to mid 1970s (Fig. 3a). Singular Spectrum Analysis (SSA-Toolkit; Dettinger et al., 1995; Vautard et al., 1992) was used to identify the Mentawai long-term $\Delta^{14}C$ trend resulting from the influx of bomb-laden ^{14}C from the atmosphere into the upper ocean (Fig. 3a). Applying a high-pass filter with a cut-off period of 6 years yields an equivalent time-series to the SSA long-term $\Delta^{14}C$ time-series (r=0.95). The Mentawai post-bomb peak occurs approximately 10 years after the 1963 atmospheric bomb radiocarbon peak (Nydal, 2000). The rise in $\Delta^{14}C$ in the Sumatra coral, in response to the maximum in nuclear weapons testing, is delayed by 2-3 years between 1954 and 1963 relative to the rise in coral $\Delta^{14}C$ from the coast of Kenya (Watamu; $3^{o}S$, $39^{o}E$) (Grumet et al., 2002a) (Fig. 3a,b). Thereafter, the Mentawai $\Delta^{14}C$ signal rises as a faster rate until about 1971, illustrated when the Mentawai 1^{st} derivative of the long-term trend is greater than the Watamu 1^{st} between 1963 and 1971 (Fig. 3b). The two records converge in the early 1970s and show similar post-bomb peak values.

Both coral $\Delta^{14}C$ time series have achieved nearly identical peak amplitudes by 1975, and the decay rates for each curve are quite similar thereafter.

Interannual Variability

The long-term trend was subtracted from the original time-series in order to isolate the annual to interannual variability in $\Delta^{14}C$ (Fig. 4). The interannual signal prior to the 1960s is on average 10‰. This range increases in the early 1960s and for the majority of the remaining portion of the record to values in excess of 20‰. Bimonthly AMS $\Delta^{14}C$ measurements on the Mentawai coral reveal mainly interannual variability with minor seasonal variability. The statistically significant (99% confidence interval) principal components of the interannual signal have a periodicity range between 2 to 5 years. In contrast, the annual cycle is significantly weaker. These results are confirmed by evolutionary Wavelet Analysis (Torrence, and Compo, 1998).

Discussion

Pre-bomb and Source Water

In order to determine possible source areas contributing depleted ^{14}C to the coast of Sumatra, we compared pre-bomb values from the surrounding waters to the Mentawai pre-bomb coral value. Bivalve and gastropod specimens sampled in the Bay of Bengal (Dutta et al., 2001), coral samples from the Pirotan Island, Gulf of Kutch (Bhushan et al., 1994) and a gastropod sample from the South coast of Java (Southon et al., 2002) report an average pre-bomb value of -56‰±1 (Fig. 1a). The Mentawai pre-bomb average of -64‰ is depleted by ~10‰ relative to these specimens. The difference in pre-bomb average values between these sites and the Mentawai coral site can be explained by local oceanography. For example, in the Bay of Bengal, the large amount of freshwater input

from the major rivers causes a steep gradient of the isopycnals, preventing advection of deeper ^{14}C depleted water (Milliman and Meade, 1983; Dutta et al., 2001). In the Gulf of Kutch where the average water depth is less than 30 m, the surface waters equilibrate faster with atmospheric CO_2 resulting in a less depleted pre-bomb average from Pirotan Island (Bhushan et al., 1994). In a similar manner, Southon et al. (2002) explain higher pre-bomb $\Delta^{14}C$ from the south coast of Java as well as along the west coast of Australia as mixing with well-equilibrated water from the far western and southwestern Pacific via the Indonesian Throughflow (ITF). This comparison, illustrating relatively enriched pre-bomb values from the Bay of Bengal, the Gulf of Kutch in the Arabian Sea and the South coast of Java relative to the Mentawai pre-bomb value, suggests that the respective surrounding waters are not sources of depleted ^{14}C to the coast of Sumatra. We therefore explore possible source areas by examining transport pathways from the Arabian Sea and the Pacific Ocean.

The Arabian Sea gyre helps propagate deep Indian Ocean water throughout the northern and equatorial Indian Ocean. For example, Southon et al. (2002) suggests that southeastward flow from Arabian Sea extends as far east as 80 to 100ºE south of the equator to Cocos-Keeling at 12ºS, 97ºE. They conclude that elevated marine reservoir age correction (ΔR) values from Ceylon, Sri Lanka, are consistent with southeast transport of radiocarbon-depleted Arabian Sea Water. These samples yield a pre-bomb average of -65‰, which is consistent with our calculated pre-bomb average from the coast of Sumatra. However, the higher salinity (S>34.7 psu) and lower oxygen concentration (O_2 2.0 ml l^{-1}) characteristic of North Indian Ocean Water is found between

300-800 m in the eastern Indian Ocean (Fieux et al., 1994). Thus, North Indian Ocean water is not a source of depleted $\Delta^{14}C$ to the coast of Sumatra since it is too deep.

Another possible source area is the Pacific Ocean with waters traveling in the ITF. Water masses from the Pacific Ocean traveling in the ITF will have a tendency to flow westward across the basin due to conservation of vorticity (Cane and Molnar, 2001). This is confirmed by observations showing that the majority of ITF transport is between 7º and 15ºS (Fieux et al., 1994; Wijffels et al., 2002) (Fig. 1). We would not expect the Indonesian Seas to be a source region for depleted-^{14}C water to the coast of Sumatra. Therefore, we argue that depleted-^{14}C water off Sumatra is locally derived and also exported from the coast of Java where the northwest propagation of the upwelling center is controlled by the strength of alongshore winds and the Coriolis effect (Susanto et al., 2001). Furthermore, the lack of seasonal structure in the pre-bomb period suggests that these upwelling events are episodic rather than seasonal.

Rapid mixing between the surface and subsurface along the coast of Sumatra can also explain differences in the pre-bomb averages between the Kenyan and Sumatran coral sites. As reported earlier, the decrease in Mentawai pre-bomb average from 1877 to 1954 is less than 2‰. This is barely distinguishable from the calculated standard error of ~1‰. These results suggest a minimal Suess effect, a lowering of atmospheric $\Delta^{14}C$ to negative values prior to the 1950s through fossil fuel burning (Stuiver and Quay, 1981), at the Mentawai site. The influence of deeper, older water in the eastern Indian Ocean relative to the western Indian Ocean is seen in sections of anthropogenic CO_2 along 57ºE and 92ºE (Sabine et al., 1999). Compression and shoaling of isopycnal surfaces occur along 92ºE facilitates mixing of deeper, depleted ^{14}C water in the eastern Indian Ocean

and helps explain the modulated Suess effect. In comparison to Mentawai, Grumet et al. (2002b) applied a 10‰ Suess correction to the Kenyan pre-bomb $\Delta^{14}C$ record. Applying this correction yields a Kenya pre-bomb average of -50‰. In contrast, the Mentawai pre-bomb record exhibits a more depleted pre-bomb average, -64‰. Assuming appropriate Suess corrections have been applied at both sites, the steady state pre-bomb distribution is offset by almost 15‰ across the equatorial Indian Ocean (Fig. 5). Thus, differences during the steady state pre-bomb suggest that rapid mixing at the Mentawai site leads to a greater influence of deeper, older water depleted in ^{14}C.

Long Term Trend and Intrabasin Comparison

The Mentawai and Kenya $\Delta^{14}C$ coral time-series display a synchronous response to the input of nuclear bomb ^{14}C in the mid-1950s (Fig. 3a). However, the Kenya record rises at a much faster rate during the influx of maximum bomb ^{14}C. As a result, the Kenyan $\Delta^{14}C$ record leads the Mentawai record by 2-3 years from 1954 to 1963 (Fig 3a). Uncertainties in the chronology could conspire to produce such a phase lead/lag relationship. However, we have spent considerable time developing the chronologies for the coral $\Delta^{14}C$ records and believe their chronologies to be robust. Therefore, the primary cause for difference in $\Delta^{14}C$ records is either a difference in atmospheric $^{14}CO_2$ signal or varying degrees of entrainment of depleted ^{14}C subsurface water into the surface which causes differences in the slope of $\Delta^{14}C$ vs. time. The slow exchange rate between atmospheric CO_2 molecules with the upper ocean (~7-10 years), allows $^{14}CO_2$ molecules produced by bomb testing to become nearly homogenized within the atmosphere (Toggweiler et al., 1989). Therefore, we argue that the different sites have different rise rates due to relative difference in input from radiocarbon depleted thermocline water

relative to the input from gas exchange with the atmosphere. Furthermore, in areas that are influenced by horizontal transport of water and very little upwelling, $\Delta^{14}C$ values rise more quickly (Druffel, 1996). The dominance of horizontal advection along the coast of Kenya is shown in Grumet et al.'s (2002b) work where the Watamu coral $\Delta^{14}C$ time-series responds to meridional transport in the western Indian Ocean due to the monsoon reversal of the Somali Current.

Druffel (1989) observed a similar lag in a Bermuda coral $\Delta^{14}C$ record relative to a record from Florida. According to that study, mixing and subsequent storage of bomb radiocarbon in the upper few hundred meters of the water column of the Sargasso Sea results in the dilution of the bomb radiocarbon signal in the surface layer. In contrast, the Gulf Stream does not experience deep convective mixing (e.g., rapid exchange between the surface and subsurface layers) and bomb radiocarbon is concentrated in the shallow mixed layer. As a consequence, the rate of water mass renewal (e.g., ventilation rate) is slower in the Sargasso Sea (Druffel, 1989; 1996). In a similar manner, we propose that convective mixing (e.g., exchange between surface and subsurface layers) is stronger in the eastern Indian Ocean than along the coast of Kenya and exhibits a slower water mass renewal rate relative to the western Indian Ocean. As mentioned earlier, rapid mixing between the surface and subsurface along the coast of Sumatra can also explain differences in the pre-bomb averages between the eastern and western Indian Ocean coral sites.

Following the rapid rise in surface $\Delta^{14}C$ off the coast of Kenya during the 1960s, the Mentawai and Watamu $\Delta^{14}C$ records converge in the early 1970s, with slightly enriched values in the Mentawai record until about 1975 when both records have

achieved nearly identical peak amplitudes, and the decay rates for each curve are quite similar thereafter. The rate increase of $\Delta^{14}C$ at Sumatra from about 1963 to 1971 relative to the increase at Watamu, as illustrated in the change of the first of the long-term trend (Fig. 3b), reflects basin wide differences in lateral and vertical mixing. For example, greater meridional transport of ^{14}C-depleted water from enhanced upwelling off the coasts of Oman and Somali to the coast of Kenya would act to decrease the rise of $\Delta^{14}C$ vs. time. In contrast, a reduction of upwelling events off the coast of Sumatra due to weaker easterlies would be reflected as an increase in the rate of coral $\Delta^{14}C$ vs. time. Thus, during this decade when the coral $\Delta^{14}C$ records are out of phase, the western and eastern sides of the equatorial Indian Ocean are experiencing opposite upwelling conditions.

In comparison, in the Ocean surface $\Delta^{14}C$ values from a Galapagos coral $\Delta^{14}C$ record (0, 90ºW) are attenuated relative to those on the western side of the Pacific (Guilderson et al., 1998). Pacific thermocline waters off the coast of Peru ventilate every 10-15 years (Jenkins, 1987; Toggweiler et al., 1991). Our results suggest that the thermocline waters upwelling in the Sumatra region are being fed by waters that are more recently exposed to the atmosphere and have a shorter residence time compared to the eastern Pacific Ocean. For example, in the early Mentawai coral $\Delta^{14}C$ record water upwelled along the coast of Sumatra is largely devoid of bomb ^{14}C which helps dilute surface $\Delta^{14}C$ values. However, later in the record the upwelled water becomes saturated with bomb ^{14}C input such that the rate of $\Delta^{14}C$ rise accelerates in the early 1970s. In comparison to the Pacific Ocean, we argue that thermocline waters ventilate every 2-3

years off the coast of Sumatra. In the following section, we use calculations from a box model to test this water mass renewal rate.

Box Model Calculation

A multibox isopycnal mixing model (Druffel 1989; Druffel, 1997) was employed to estimate the water mass renewal rate (e.g., ventilation rate of the upper water column) off the coast of Sumatra. A schematic of this model is shown in Figure 6. The model contains an atmospheric box (A) with annual $\Delta^{14}C$ values of atmospheric CO_2 (from tree rings) reported from Stuiver and Quay (1981) during the pre-bomb and Manning and Melhuish (1994) of atmospheric CO_2 during the post-bomb period. The rate of output of $^{14}CO_2$ from the sea surface to the air, k_1, is a function of the averaged mixed layer depth Z (25 m; Levitus, 1982) and the ΔCO_2 in the surface waters (2.0 mol of CO_2 m^{-3}; Levitus, 1982) where:

$$k_1 = I/Z * \Delta CO_2$$

The CO_2 gas exchange rate (I) (6.4 mol of CO_2 m^{-2} $year^{-1}$) is a function of CO_2 concentration is seawater (0.019mM at an average temperature of 25ºC) and the gas exchange piston velocity (Vp) (m/d/y), where:

$$I = Vp * 0.019\ mM * 365\ d/yr$$

The gas exchange piston velocity is a function of wind speed (WS) (Jenkins, 1988) according to:

$$V_p = WS * 0.9995 - 3.47$$

The annual wind speed at the Sumatra site is 4.4 m/s (Slutz et al., 2985). The input of $^{14}CO_2$ to the ocean F(t), is a function of the difference between both the partial pressure

of CO_2 (pCO_2) and the atmospheric and surface water $^{14}C/^{12}C$ ratios ($\Delta^{14}C_{s,a}$) according to:

$$F(t)=\frac{[\Delta^{14}C_a/0.983-\Delta^{14}C_s*(pCO_{2s}/pCO_{2a})]}{(\Delta^{14}C_a/0.983-\Delta^{14}C_s)}$$

In this case, we assume $pCO_{2s} = pCO_{2a}$ where F(t)=1, such that the net transfer of $^{14}CO_2$ to the surface ocean is a function of the $^{14}C/^{12}C$ gradient. This assumption is close to Broecker et al.'s (1985) inventory input for the tropical Indian Ocean of 0.9. This in turn affects the input rate of $^{14}CO_2$ from the air to the sea surface, k_{-1}, where:

$$k_{-1}=F(t)* k_1/0.983 \ (yr^{-1})$$

The surface boxes K(t) and S(t) represent the Fraction Modern, as defined by Stuiver and Polach (1977), in surface waters at Kenya and Sumatra, respectively. The subsurface box at Sumatra, represented as D(t), is assumed to have a $\Delta^{14}C$ value of -100‰ during the pre-bomb period (Stuiver and Ostlund, 1983) There is no local upwelling along the coast of Kenya (Grumet et al., 2002b), therefore we have not included a subsurface box at this site. Convective mixing between the surface waters at Sumatra (S) and the subsurface box (D) is a function of the water mass renewal rate (W). The $\Delta^{14}C$ value at Sumatra is affected by input from boxes K(t), A(t) and D(t). The zonal contribution of Kenya surface water, via the South Equatorial Counter Current (SECC) during the winter monsoon, is estimated at 30% relative to the vertical component at Sumatra, assuming the SECC transport is 5 Sv and offshore Ekman transport is 15 Sv (Schott and McCreary, 2001; Schott et al., 2002). Increasing (decreasing) the contribution from Kenya increases (decreases) the surface $\Delta^{14}C$ values at Sumatra, as

would be expected since the pre-bomb values off the coast of Kenya are enriched relative to Sumatra (Grumet et al., 2002a).

We solved for $S(t+\Delta t)$ using the steady-state pre-bomb $\Delta^{14}C$ coral values at Sumatra and Kenya, -50‰ and -64‰, respectively and a subsurface value of -100‰ where

$$S(t+\Delta t)=S(t)+0.30*\Delta t[K(t)-S(t)]+\Delta t*[k_{-1}*A(t+\Delta t)- k_1*S(t)]+\Delta t*W*[D(t+\Delta t)-S(t)]$$

At a time-step of 0.20 years a constant annual value for W of 0.40 yr^{-1} , or 2.5 years, is required in order to satisfy the pre-bomb steady state conditions. To test the sensitivity of the model-calculation to changes in the input from Kenya, we ran the model with no zonal contribution, which yielded a water mass renewal rate of 3.5 years. In contrast, if W is equal to 0, Sumatra surface values are -43‰ despite increasing the zonal contribution from Kenya to 100%, suggesting that isopycnal mixing between the surface and subsurface box is an essential process off the coast of Sumatra in determining surface $\Delta^{14}C$ values. Results of the forward calculation are shown in Figure 6a with a constant W=0.44 yr^{-1}. The fact that the model-calculated surface $\Delta^{14}C$ at Sumatra correlates to the observed data (r=0.98; σ=0.95) between 1955 and 1970 (Fig. 6b) suggests that a water mass renewal rate of between 2-3 years can help explain the lead-lag relationship between the Watamu and Mentawai $\Delta^{14}C$ time-series when the two coral records deviate (Fig. 3). The correlation between the model calculated surface $\Delta^{14}C$ values and coral data is weaker later in the record. We attribute this to the poor constraint on subsurface $\Delta^{14}C$ values where we used limited hydrographic data from GEOSECS (Stuiver and Ostlund,

1983) and WOCE (Key et al., 2002) to calculate a change in subsurface $\Delta^{14}C$ vs. time of ~0.20‰/yr.

Short Term Trend

The lack of a pronounced seasonal signal can be explained by examining the seasonal oceanography. Although the seasonal cycle of the SJC is dictated by the seasonally reversing monsoons, the SJC is predominantly southeastward between the equator and 104ºE throughout the year (Quadfasel and Cresswell, 1992). In contrast, between Java and Sumba the SJC reverses direction. Unlike the Watamu $\Delta^{14}C$ signal which is sensitive to monsoonal reversals in the SC, the Mentawai site is not responsive to reversing boundary currents associated with the SJC. Furthermore, during the SE monsoon, time-longitude SST data along the coast of Java-Sumatra indicate that the northwestward upwelling center is greatly reduced westward of 105^{o}E and alongshore winds are at a maximum at 105ºE (Susanto et al., 2001). These observations along with the absence of a distinct annual coral $\Delta^{14}C$ signal suggest that the Mentawai coral site, at 98ºE, is too far east to capture upwelling associated with the seasonally reversing monsoons. Therefore, the interannual coral $\Delta^{14}C$ signal is not masked or complicated by a seasonal signal. Instead, the Mentawai Islands appear to be influenced by extreme events, such as those documented during anomalous easterlies (Behera et al., 1999; Yu and Reinecker, 1999; 2000; Murtugudde et al., 2000; Vinayachandran et al., 1999).

Spectral analysis of the de-trended time series, using a multi-taper method (SSA-Toolkit; Vautard et al., 1992; Dettinger et al., 1995), reveals the dominance of a ~3 year ENSO like periodicity (Fig. 7). In contrast, the annual cycle is significantly weaker at the 99% confidence interval using a white-noise spectrum. Interannual modes of SST, sea-

level variability, upper-ocean heat content and surface wind stress in the Indian Ocean are also found in numerous instrumental records (e.g., Tourre and White, 1997; Qian et al., 2002) and modeling studies (e.g., Murtugudde et al., 1998; Murtugudde and Busalachhi, 1999). For example, Potemra and Lukas (1999) document a dominant interannual signal, with the annual signal being secondary, in sea-level variability based on TOPEX/Poseidon satellite data from 1992 to 1998. Likewise, upwelling along the coast of Java and Sumatra is characterized by significant interannual variability as revealed by hydrographic and XBT/MBT data from 1970 to 2000 (Susanto et al., 2001).

Using SST and upper-ocean heat content (HCA) fields and surface wind stress data from 1958-1998, Huang and Kinter (2002) applied empirical orthogonal function (EOF) analysis to analyze the interannual variability in the tropical ocean. They found the 1st EOF to be characterized by contrasting HCA in the east and west basins, a corresponding equatorial SST zonal gradient, and anomalous easterly winds in the central and eastern equatorial Indian Ocean with along-shore components near the eastern coast (Huang and Kinter, 2002). Their leading mode of interannual variability in the Indian Ocean represents a coupled ocean-atmosphere characterized by zonal gradients. Oscillatory patterns of the 1st EOF are centered around 2 and 4 years. Their results suggest a strong link between Indian Ocean interannual variability and ENSO, especially between 1976 and 1998. A SST record derived from Sr/Ca coral measurements from Christmas Island (10ºS, 105ºE) also indicates a strong teleconnection between the tropical Indian and Pacific Oceans (Marshall and McCulloch, 2001). Annamalai et al. (2003) propose that ENSO-related changes in the eastern equatorial Indian Ocean are in response to atmospheric changes linked to a change in the Walker circulation where upwelling

favorable winds off Java and Sumatra are enhanced as a response to the development of an anticyclone over the southeastern Indian Ocean. Therefore, it may be possible that the Mentawai $\Delta^{14}C$ interannual variability is related to the structural change observed in the Indo-Pacific Ocean basin.

Conclusions

Our intrabasin comparison between coral $\Delta^{14}C$ records from the coasts of Sumatra and Kenya reveals a distinct difference in water mass mixing processes across the equatorial Indian Ocean basin. In the western equatorial Indian Ocean, surface waters are in contact with the atmosphere for a longer period of time and there is less entrainment of depleted ^{14}C water from the subsurface. In contrast, wind-induced upwelling and rapid mixing along the coast of Sumatra entrains ^{14}C-depleted water from the subsurface, which dilutes the effect of the uptake of bomb-laden ^{14}C by the surface-ocean. As a result, the rise in coral $\Delta^{14}C$ values at the Sumatra site are delayed by 2-3 years during the maximum input of bomb produced radiocarbon relative to the rise at the Kenya site ^{14}C. Furthermore, differences during the steady state pre-bomb also suggest that rapid mixing at the Mentawai site leads to greater influence of deeper, older water depleted in ^{14}C. Results from a multibox model suggest that a water mass renewal rate of between 2 and 3 years can help explain the lead-lag relationship between the rise in the Watamu and Mentawai $\Delta^{14}C$ coral records. Bimonthly AMS $\Delta^{14}C$ measurements on the Mentawai coral reveal mainly interannual variability with minor seasonal variability. The interannual signal may be a response to changes in the Walker circulation, the development of easterly wind anomalies, shoaling of the eastern thermocline, and

upwelling of ^{14}C-depleted water along the coast of Sumatra. These results support the notion of a link between ocean-atmosphere dynamics in the Pacific and Indian Oceans.

Acknowledgements

We thank D. Prayudi, I. Suprianto, K. Glenn, T. Watanabe, K. Sieh and the Indonesian Institute of Sciences (LIPI) for logistical support and technical assistance with coral drilling in Sumatra. H. Scott-Gagan and J. Cali are gratefully acknowledged for assistance with the stable-isotope mass spectrometry and L. Hewitt T. Lange for assistance with AMS sample preparation. A portion of this work was performed under the auspices of the U.S. Department of Energy by the University of California Lawrence Livermore National Laboratory (contract W-7405-Eng-48).

References:

Abram, N.J., M.K. Gagan, M.T. McCulloch, J. Chappell, and W.S. Hantoro, Coral reef death during the 1997 Indian Ocean Dipole linked to Indonesian wildfires, *(in press, Science)*.

Allan, D. Chambers, W. Drosdowsky, H. Hendon, M. Latif, N. Nicholls, I. Smith, R. Stone, and Y. Tourre, Is there an Indian Ocean dipole, and is it independent of the El Niño - Southern Oscillation? *CLIVAR Exchanges, 6*, 18-22, 2001.

Annamalai, H., R. Murtugudde, J.T. Potemra, S.P. Xie, and B. Wang, Coupled dynamics in the Indian Ocean: Externally or internally forced? *Deep Sea Res. Part I*, *50*, 2305-2330, 2003.

Bard, E., M. Arnold, H. G. Ostlund, P. Maurice, P. Monfray, and J.-C. Duplessy, Penetration of bomb radiocarbon in the tropical Indian Ocean measured by means of accelerator mass spectrometry, *Earth Planet. Sci. Lett., 87,* 379-389, 1988.

Behera, S.K., R. Krishnan, and T. Yamagata, Unusual ocean-atmosphere conditions in the tropical Indian Ocean during 1994, *Geophys. Res. Lett., 26,* 3001-3004, 1999.

Bhushan, R., S. Chakraborty, and S. Krishnaswami, Physical Research Laboratory (Chemistry) Radiocarbon Date List-I, *Radiocarbon, 36*, 251-256, 1994.

Broecker, W.S., T.H. Peng, G. Ostlund, and M. Stuiver, The distribution of bomb radiocarbon in the ocean, *J. Geophys. Res., 90*, 6953-6970, 1985.

Brown, T.A., G.W. Farwell, P.M. Grootes, F.H. Schmidt, and M. Stuiver, Intrannual variability of the radiocarbon content of corals from the Galapagos-Islands, *Radiocarbon, 35,* 245-251, 1993.

Cane, M. and P. Molnar, Closing of the Indonesian seaway as a precursor to east African aridircation around 3-4 million years ago, *Nature 411,*157-162, 2001.

Clarke, A. and X. Liu, Interannual sea-level in the northern and eastern Indian Ocean, *J. Phys. Oceanogr. 24,* 1224-1235, 1994.

Dettinger, M.D., M. Ghil, C.M. Strong, W. Weibel, and P. Yiou, Software expedites singular-spectrum analysis of noisy time series, *EOS Trans, AGU, 76,* 12-14, 1995.

Donahue, D.J., A.J.T. Jull, and L.J. Toolin, Radiocarbon measurements at the University of Arizona AMS Facility, *Nucl. Instrum Methods Phys. Res., Sect., 52,* 224-228, 1990.

Druffel, E.M., Post-bomb radiocarbon records of surface corals from the tropical Atlantic Ocean, *Radiocarbon, 38,* 563-572, 1996.

Druffel, E. M., Banded corals: Changes in oceanic ^{14}C during the Little Ice-Age, *Science, 218*, 13-19, 1982.

Druffel, E.M. and T.W. Linick, Radiocarbon in annual coral rings of Florida, *Geophys. Res. Lett., 5,* 913-916, 1978.

Druffel, E.M., Bomb radiocarbon in the Pacific: Annual and seasonal timescale variations, *J. Mar. Res., 45,* 667-698, 1987.

Druffel, E.M., Decade time scale variability of ventilation in the North-Atlantic: High-precision measurements of bomb radiocarbon in banded corals, *J. Geophys. Res., 94*, 3,271-3,285, 1989.

Druffel, E.M., Post-bomb radiocarbon records of surface corals from the tropical Atlantic Ocean, *Radiocarbon, 38*, 563-572, 1996.

Druffel, E.M., Geochemistry of corals: Proxies of past ocean chemistry, ocean circulation, and climate, *Proc. of the Natl. Academy Sciences,, 94,* 8,354-8,361, 1997.

Druffel, E.M., Pulses of rapid ventilation in the North Atlantic surface ocean during the past century, *Science, 275,* 1,454-1,457, 1997.

Dutta, K., R. Bhushan, and B.L.K. Somayajulu, Delta R correction values for the northern Indian Ocean, *Radiocarbon 43,* 483-488, 2001.

Feng, M., G. Meyers, and S. Wijffels, Interannual upper ocean variability in the tropical Indian Ocean, *Geophys. Res. Lett., 28*, 4,151-4,154, 2001.

Fieux, M., C. Andrie, P. Delecluse, A.G. Ilahude, A. Kartavtseff, F. Mantisi, R. Molcard, and J.C. Swallow, Measurements within the Pacific Indian Oceans throughflow region, *Deep Sea Res. Part I, 41,* 1091-1130, 1994.

Gagan, M.K., A.R. Chivas, and P.J. Isdale, High-resolution isotopic records from corals using ocean temperature and mass-spawning chronometers. *Earth Planet. Sci. Lett., 121*, 549-558, 1994.

Gagan, M.K., L.K. Ayliffe, D. Hopley, J.A. Cali, G.E. Mortimer, J. Chappell, M.T. McCulloch, and M.H. Head, Temperature and surface-ocean water balance of the mid-Holocene tropical western Pacific, *Science, 279*, 1014-1018, 1998.

Godfrey, J.S., The effect of the Indonesian throughflow on ocean circulation and heat exchange with the atmosphere: A review, *J. Geophys. Res., 101,* 12,217-12,237, 1996.

Grumet, N. S., R. B. Dunbar and J. E. Cole, Multisite record of climate change from Indian Ocean corals. Proceedings 9th International Coral Reef Symposium, Bali, Indonesia, 1: 359-364, 2000.

Grumet, N., T.P. Guilderson, and R.B. Dunbar, Meridional transport in the Indian Ocean traced by coral radiocarbon, *J. Mar. Res., 60,* 725-742, 2002a.

Grumet, N.S., T.P. Guilderson and R.B. Dunbar, Pre-bomb radiocarbon variability inferred from a Kenyan coral record, *Radiocarbon, 44,* 581-590, 2002b.

Guilderson, T. P. and D. P. Schrag, Abrupt shift in subsurface temperatures in the tropical Pacific associated with changes in El Nino, *Science, 281,* 240-243, 1998.

Guilderson T.P., K. Caldeira, and P.B. Duff, Radiocarbon as a diagnostic tracer in ocean and carbon modeling, *Global Biogeochem. Cycles, 14*, 887-902, 2000.

Hastenrath, S., Dipoles, temperature gradients, and tropical climate anomalies, *Bull. Amer. Meterol. Soc., 83,* 735-738, 2002.

Huang, B. and J. Kinter, Interannual variability in the tropical Indian Ocean, *J. Geophys. Res., 107,* 3,199-3226, 2002.

Jenkins, W.J., ^{3}H and ^{3}He in the Beta Triangle: Observations of gyre ventilation and oxygen utilization rates, *J. Phys. Oceanogr. 17*, 763-783, 1987.

Jenkins, W.J., The nitrate flux into the euphotic zone near Bermuda, *Nature, 331*, 521-523, 1988.

Jenkins, W.J. and W.M. Smethie, Transient tracers track ocean climate signals, *Oceanus, 39*, 29-32, 1996.

Jull, A., D. Donahue, A.L. Hatheway, T.W. Linick, and L.J. Toolin, Production of graphite targets by deposition from CO/H-2 for precision accelerator ^{14}C measurements, *Radiocarbon*, *28*, 191-197, 1986.

Key, R.M. and P.D. Quay, U.S. WOCE Indian Ocean Survey, Final Report for radiocarbon, Ocean Tracers Laboratory, Tech. Rep. # 02-1.Atmospheric and Oceanic Sciences Program, Princeton Univ., Princeton, NJ, 2002.

Levitus, S., Climatological Atlas of the World Ocean. NOAA Prof. Pap. No. 13, U.S. Govt. Print. Office, Washington, D.C., 173 p., 1982

Linick, T., A. Jull, L.J. Toolin, and D.J. Donahue, Operation of the NSF-Arizona Accelerator Facility for radioisotope analysis and results from selected collaborative research projects, *Radiocarbon*, *28*, 522-533, 1986.

Linsley B.K., R.G. Messier, and R.B. Dunbar, Assessing between-colony oxygen isotope variability in the coral *Porites lobata* at Clipperton Atoll, *Coral Reefs, 18*, 13-27, 1999.

Manning, M.R. and W.H. Melhuish, Atmospheric Δ^{14}C record from Wellington, In Trends: A Compendium of Data on Global Change, Carbon Dioxide Information Analysis Center, Oak Ridge National Laboratory, U.S. D.O.E., Oak Ridge, Tenn., U.S.A., 1994.

McConnaughey, T., ^{13}C and ^{18}0 disequilibrium in biological carbonates: I Patterns, *Geochim. Cosmochim. Acta., 53*, 151-162, 1989.

Marshall, J. and M. McCulloch, Evidence of El Nino and the Indian Ocean Dipole from Sr/Ca derived SSTs for modern corals at Christmas Island, Eastern Indian Ocean, *Geophys. Res. Lett., 28,* 3,453-3,456, 2001.

Milliman, J. D. and R. H. Meade, World-wide delivery of river sediment to the oceans, *J. Geol. 91,* 1-21, 1983.

Murtugudde, R. and A. Busalacchi, Interannual variability of the dynamics and thermodynamics of the tropical Indian Ocean, *J. Clim. 12*, 2,300-2,326, 1999.

Murtugudde, R., A. J. Busalacchi, and J. Beauchamp, Seasonal-to-interannual effects of the Indonesian throughflow on the tropical Indo-Pacific Basin, *J. Geophys. Res., 103*, 21,425-21,441, 1998.

Murtugudde, R., J. P. McCreary, and A.J. Busalacchi, Oceanic processes associated with anomalous events in the Indian Ocean with relevance to 1997-1998, *J. Geophys. Res., 105,* 3,295-3,306, 2000.

Nydal, R., Radiocarbon in the ocean, *Radiocarbon, 42*, 81-98, 2000.

Ostlund, H.G. and C. Grall, Indian Ocean radiocarbon: Data from the INDIGO 1, 2, and 3 cruises. Oak Ridge, TN, Oak Ridge National Laboratory, 1991.

Potemra, J. T. and R. Lukas, Seasonal to interannual modes of sea level variability in the western Pacific and eastern Indian Oceans, *Geophys. Res. Lett., 26,* 365-368, 1999.

Qian, W., H. Hu, Y. Deng, and J.W. Tian, Signals of interannual and interdecadal variability of air-sea interaction in the basin-wide Indian Ocean, *Atmos.-Ocean, 40*, 293-311, 2002.

Quadfasel, D. and G.R. Cresswell, A note on the seasonal variability of the South Java Current, *J. Geophys. Res., 97,* 3685-3688, 1992.

Rao, S. A., S. K. Behera, Y. Masumoto, and T. Yamagata, Interannual subsurface variability in the tropical Indian Ocean with a special emphasis on the Indian Ocean Dipole, *Deep Sea Res. Part I, 49*,1,549-1,572, 2002.

Rhein, M., L. Stramma, and U. Send, The Atlantic deep western boundary current: Water masses and transports near the equator, *J. Geophys. Res., 100*, 2441-2457, 1995.

Rodgers, K. B., M. A. Cane, and D.P. Schrag, Seasonal variability of sea surface $\Delta^{14}C$ in the equatorial Pacific in an ocean circulation model, *J. Geophys. Res. 102,* 18,627-18,639, 1997.

Rodgers, K.B., D.P. Schrag, M.A. Cane, and N.H. Naik, The bomb 14C transient in the Pacific Ocean, *J. Geophys. Res., 105,* 8489-8512, 2000.

Sabine, C.L., R.M. Key, K.M. Johnson, F.J. Millero, A. Poisson, J.L. Sarmiento, D.W.R. Wallace and C.D. Winn, Anthropogenic CO2 inventory of the Indian Ocean, *Global Biogeochem. Cycles, 13*, 179-198, 1999.

Saji, N. H., B. N. Goswami, P.N. Vinayachandran, and T. Yamagata, A dipole mode in the tropical Indian Ocean, *Nature, 401*, 360-363, 1999.

Schott, F.A., and J.P. McCreary, The monsoon circulation of the Indian Ocean, *Progr. Ocean., 51*, 1-123, 2001.

Schott, F.A., M. Dengler, and R. Schoenefeldt, The shallow overturning circulation of the Indian Ocean, *Progr. Ocean., 53*, 57-103, 2002.

Slota, P., A. Jull, T.W. Linick, and L.J. Toolin, Preparation of small samples for ^{14}C accelerator targets by catalytic reduction of CO, *Radiocarbon, 29*, 303-306, 1987.

Slutz, R.J., S.J. Lubker, J.D. Hiscox, S.D. Woodruff, R.L. Jenne, P.M. Steurer, and J.D. Elms, Comprehensive Ocean-Atmosphere Data Set; Release 1, Climate Research Program, Boulder, Colorado, 1985.

Southon, J., M. Kashgarian, M. Fontugne, B. Metivier, and W.W.S. Yim, Marine reservoir corrections for the Indian Ocean and southeast Asia, *Radiocarbon 44,* 167-180, 2002.

Sprintall, J., J. Chong, F. Syamsudin, W. Morawitz, S. Hautala, N. Bray, and S. Wijffels, Dynamics of the South Java Current in the Indo-Australian Basin, *Geophys. Res. Lett., 26*, 2493-2496, 1999.

Sprintall, J., A.L. Gordon, R. Murtugudde, and R.D. Susanto, A semiannual Indian Ocean forced Kelvin wave observed in the Indonesian seas in May 1997, *J. Geophys. Res., 105*, 17,217-17,230, 2000.

Stuiver M, and P.D. Quay, Atmospheric ^{14}C changes resulting from fossil fuel CO_2 release and cosmic ray flux variability, *Earth Plant. Sci. Lett.,* 53, 349-362, 1981.

Stuiver, M., and H.G. Ostlund, GEOSECS Indian Ocean and Mediterranean., *Radiocarbon, 25*, 1-29, 1983.

Stuiver, M. and H.A. Polach, Discussion reporting of ^{14}C data, *Radiocarbon, 19*, 355-363, 1997.

Susanto, R.D., A.L. Gordon, and Q.N. Zheng, Upwelling along the coasts of Java and Sumatra sand its relation to ENSO, *Geophys. Res. Lett., 28,* 1599-1602, 2001.

Toggweiler, J. R., K. Dixon and K. Bryan, Simulations of Radiocarbon in a Coarse-Resolution World Ocean Model .2. Distributions of Bomb-Produced C-14, *J. Geophys. Res., 94*, 8,243-8,264, 1989.

Toggweiler, J. R., K. Dixon, and W.S. Broecker, The Peru Upwelling and the Ventilation of the South-Pacific Thermocline, *J. Geophys. Res., 96*, 2,0467-2,0497, 1991.

Tomczak, M. and J.S. Godfrey, Regional Oceanography: An Introduction. Delhi, Daya Publishing House, 2002.

Torrence, C. and G.P. Compo, A practical guide to wavelet analysis, *Bull. Am. Met. Soc., 79*, 61-78, 1998.

Tourre, Y.M. and W.B. White, Evolution of the ENSO signal over the Indo-Pacific domain, *J. Phys. Oceanogr., 27*, 683-696, 1997.

Vautard, R., P. Yiou, and M. Ghil, Singular-spectrum analysis: A toolkit for short, noisy chaotic signals, *Physica D, 58*, 95-126, 1992.

Vinayachandran, P., N. Saji, and T. Yamagata, Response of the equatorial Indian Ocean to an unusual wind event during 1994, *Geophys. Res. Lett., 26,* 1613-1616, 1999.

Webster, P. J., A. M. Moore, J.P. Loschnigg, and R.R. Leben, Coupled ocean-atmosphere dynamics in the Indian Ocean during 1997-1998, *Nature, 401,* 356-360, 1999.

Wijffels, S., J. Sprintall, M. Fieux, and N. Bray, The JADE and WOCE I10/IR6 throughflow sections in the southeast Indian Ocean. Part I: Water mass distribution and variability, *Deep Sea Res. Part I, 49,* 1341-1362, 2002.

Yamagata T., S.K. Behera, S.A. Rao, Z. Guan, K. Ashok, and H.N. Saji, The Indian Ocean dipole: A physical entity, *CLIVAR Exchanges,* **7**, 15-18, 2002.

Yu, L. and M.M. Rienecker, Mechanisms for the Indian Ocean warming during the 1997-98 El Niño, *Geophys. Res. Lett., 26,* 735-738, 1999.

Yu, L.S. and M.M. Rienecker, Indian Ocean warming of 1997-1998, *J. Geophys. Res., 105,* 16,923-16,939, 2000.

Yu, J. Y., C. R. Mechoso, J.C. McWilliams, and A. Arakawa, Impacts of the Indian Ocean on the ENSO cycle, *Geophys. Res. Lett., 29*, 1204-1204, 2002.

Figures

a)

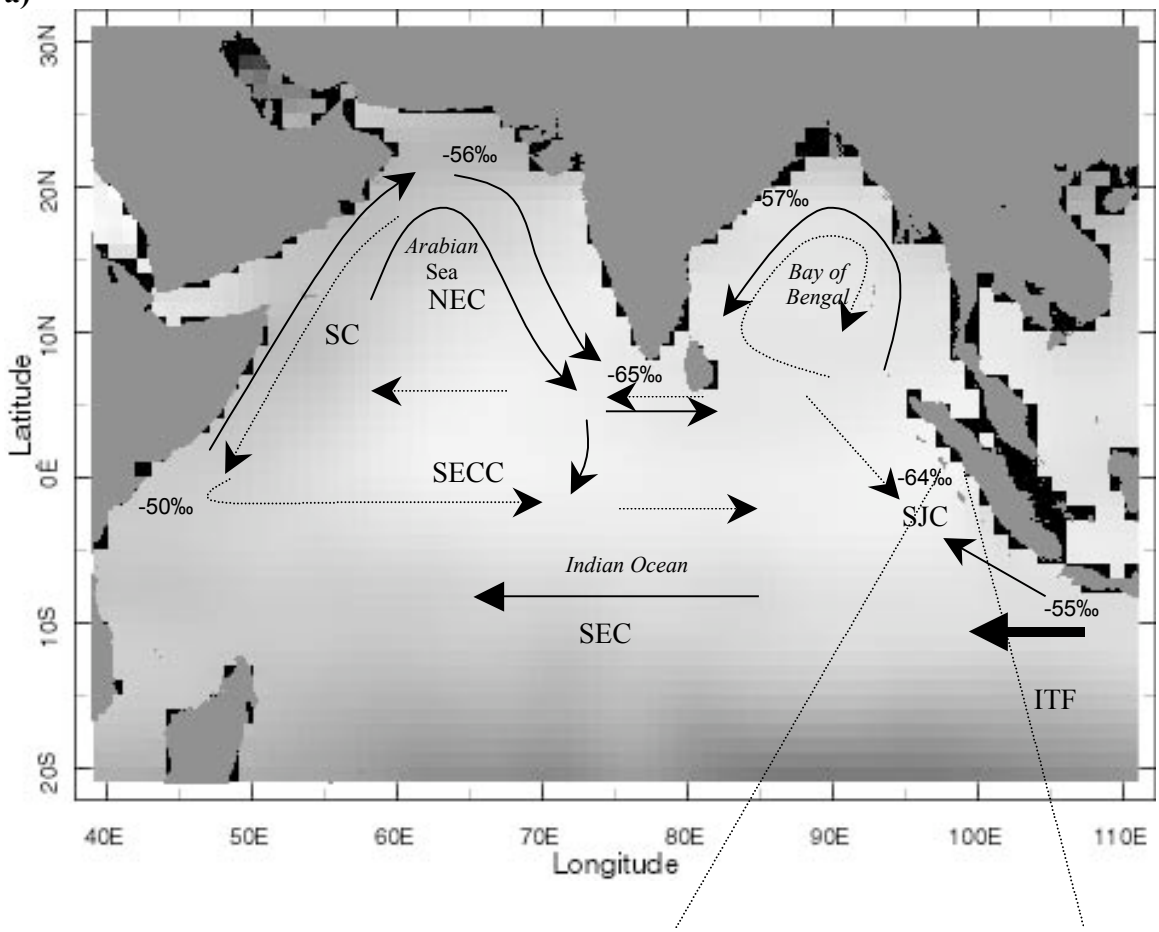
30N
20N
10N
0E
10S
20S
Latitude
40E
50E
60E
70E
80E
90E
100E
110E
Longitude
-56‰
-57‰
Arabian
Sea
NEC
SC
Bay of
Bengal
-65‰
SECC
-50‰
-64‰
SJC
Indian Ocean
SEC
-55‰
ITF

b)

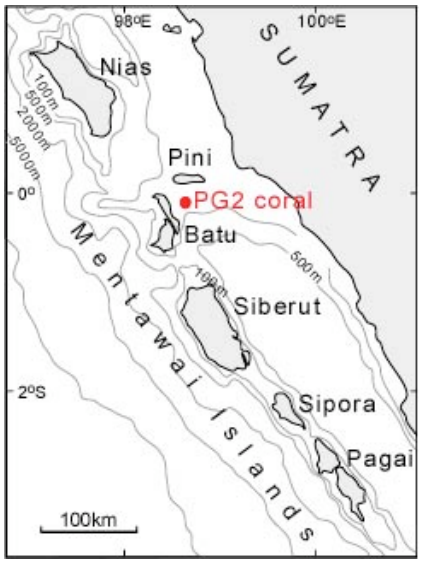
98°E
100°E
Nias
SUMATRA
100m
500m
2000m
5000m
0°
Pini
PG2 coral
Batu
500m
1000m
Siberut
Mentawai Islands
2°S
Sipora
Pagai
100km

Figure 1

a) Map of equatorial Indian Ocean depicting major current systems during the Southwest (solid arrows) and Northeast (dashed arrows) Monsoons. Significant currents include the Somali Current (SC), North Equatorial Current (NEC), South Equatorial Counter Current (SECC), South Equatorial Current (SEC), South Java Current (SJC) and the Indonesian Throughflow (ITF). Biogenic pre-bomb radiocarbon values from the south coast of Java (-55‰), Bay of Bengal (-57‰), Sri Lanka (-65‰), and Gulf of Kutch (-56‰) are labeled for comparison with this study. Coral pre-bomb coral radiocarbon values are -64‰ for Sumatra and -50‰ for Kenya. **b)** Locality map of the southwest coast of Sumatra and the Mentawai Islands. The PG2 coral collection site (0º08'S, 98º31'E) is approximately 400 m offshore of Penang Island.

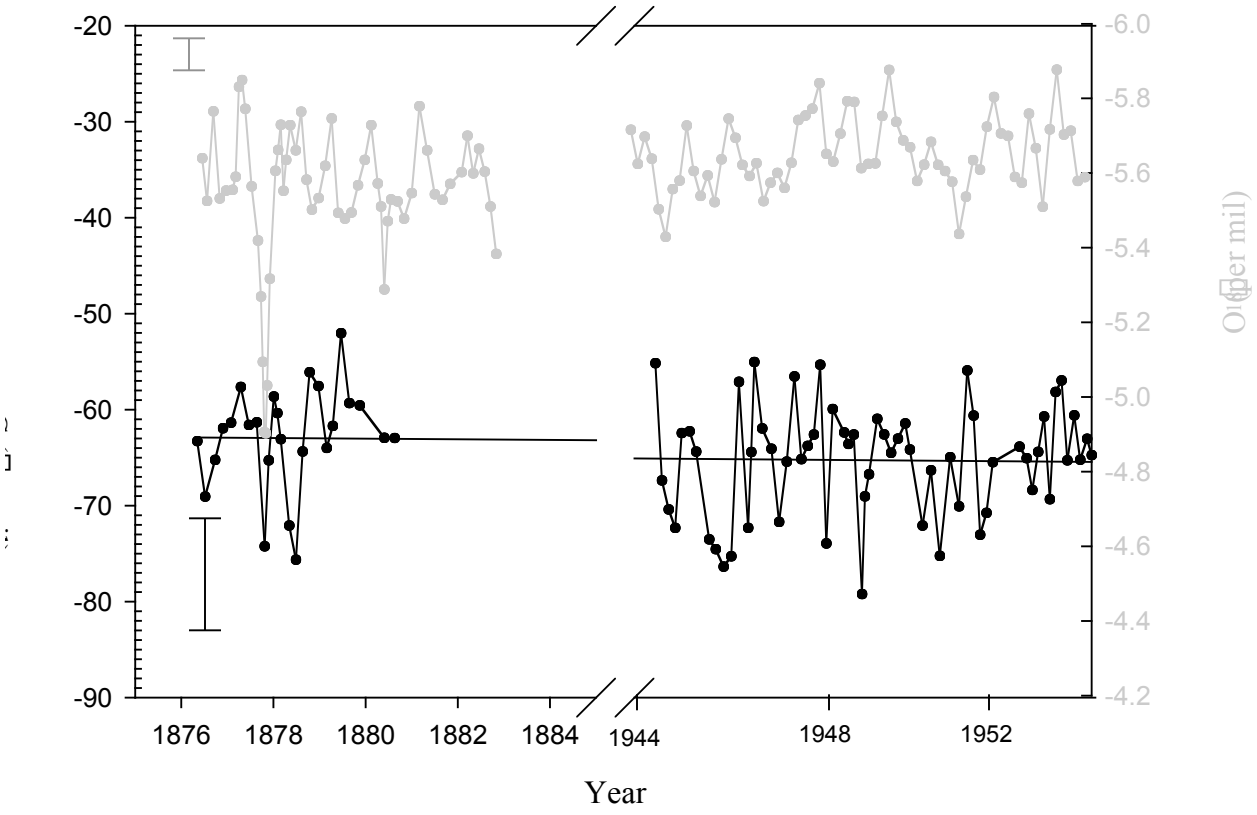

Figure 2
Pre-bomb $\Delta^{14}C$ (black curves) and $\delta^{18}O$ (grey curves; y-axis inverted) values for the Mentawai Island coral from 1876 to 1881 and 1944 to 1954. The average pre-bomb $\Delta^{14}C$ value is -64‰ with a standard error of 1‰. The change in mean coral $\Delta^{14}C$ from 1876 to 1954 (horizontal lines) is less than 2‰, indicating a negligible Suess effect in the pre-bomb Mentawai $\Delta^{14}C$ time-series.

a)

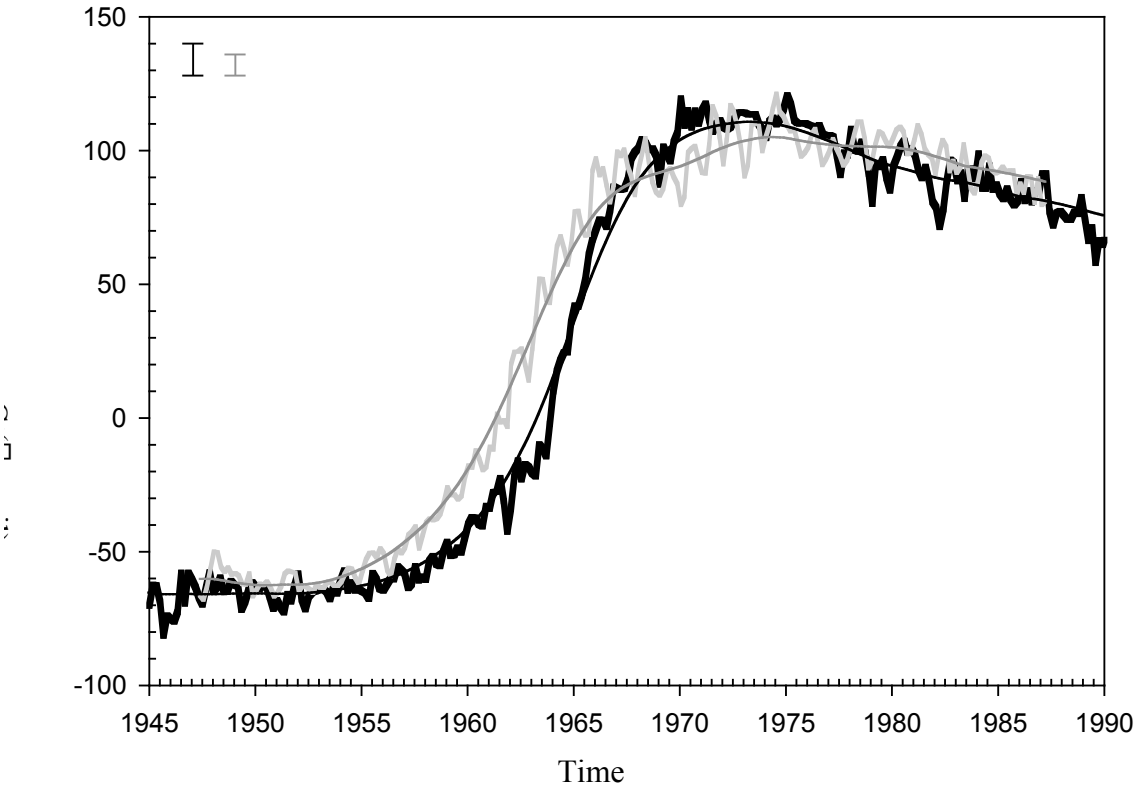
150
100
50
0
-50
-100
1945
1950
1955
1960
1965
1970
1975
1980
1985
1990
Time

b)

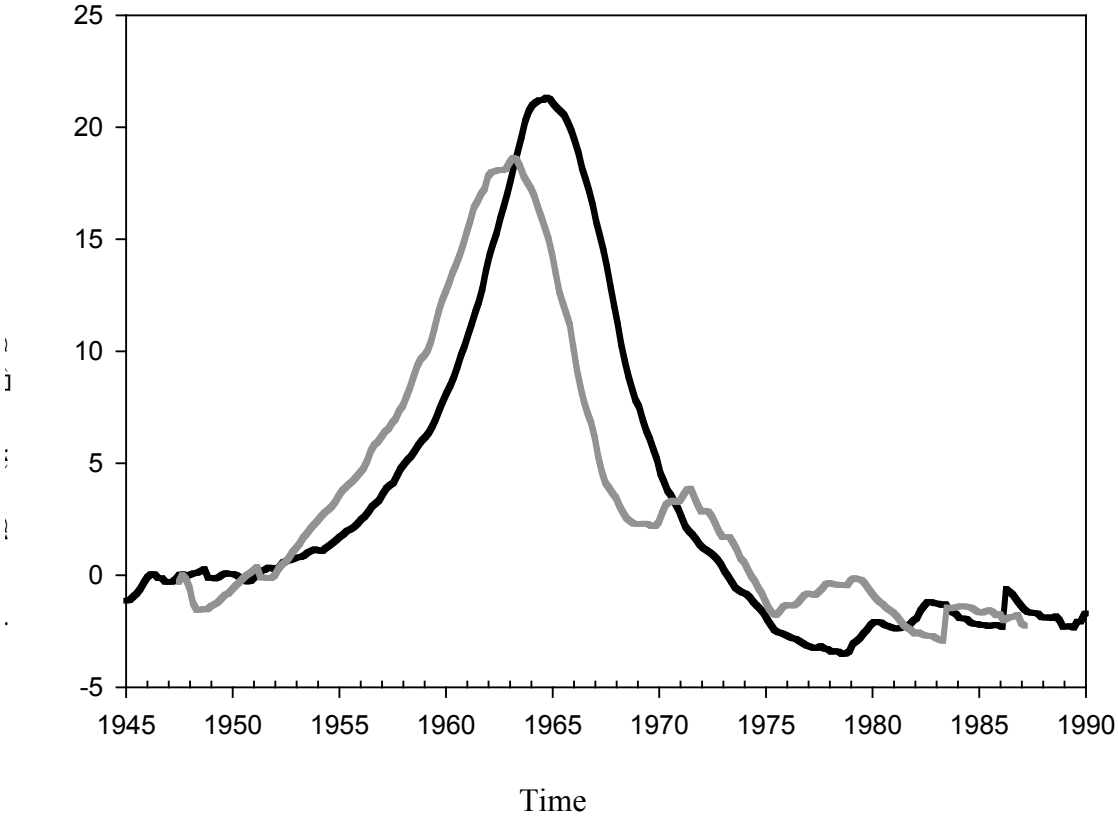

Figure 3

a) Bimonthly Mentawai (thick black line) $\Delta^{14}C$ time-series superimposed on the long-term Mentawai trend (thin black line) from 1945 to 1990. The long-term trend was calculated using singular spectrum analysis (SSA-Toolkit; Dettinger et al., 1995; Vautard et al., 1992) to isolate the leading components attributed to tenfold increase in atmospheric ^{14}C. Coral radiocarbon levels respond to atmospheric testing of nuclear weapons in the mid 1950s. The increase in $\Delta^{14}C$ recorded at Watamu (grey lines) leads the increase at the Mentawai Islands by 2-3 years during the initial rise of bomb ^{14}C between 1954 and 1963. **b)** The first derivative of the Mentawai (black) and Watamu (grey) $\Delta^{14}C$ long-term trends. The larger peak in the 1st derivative for the Mentawai coral $\Delta^{14}C$ signal indicates a relatively rapid rise in surface-ocean $\Delta^{14}C$ between 1963 and 1971. The coral $\Delta^{14}C$ records peak in the early to mid 1970s, approximately 10 years after the atmospheric maximum in 1963.

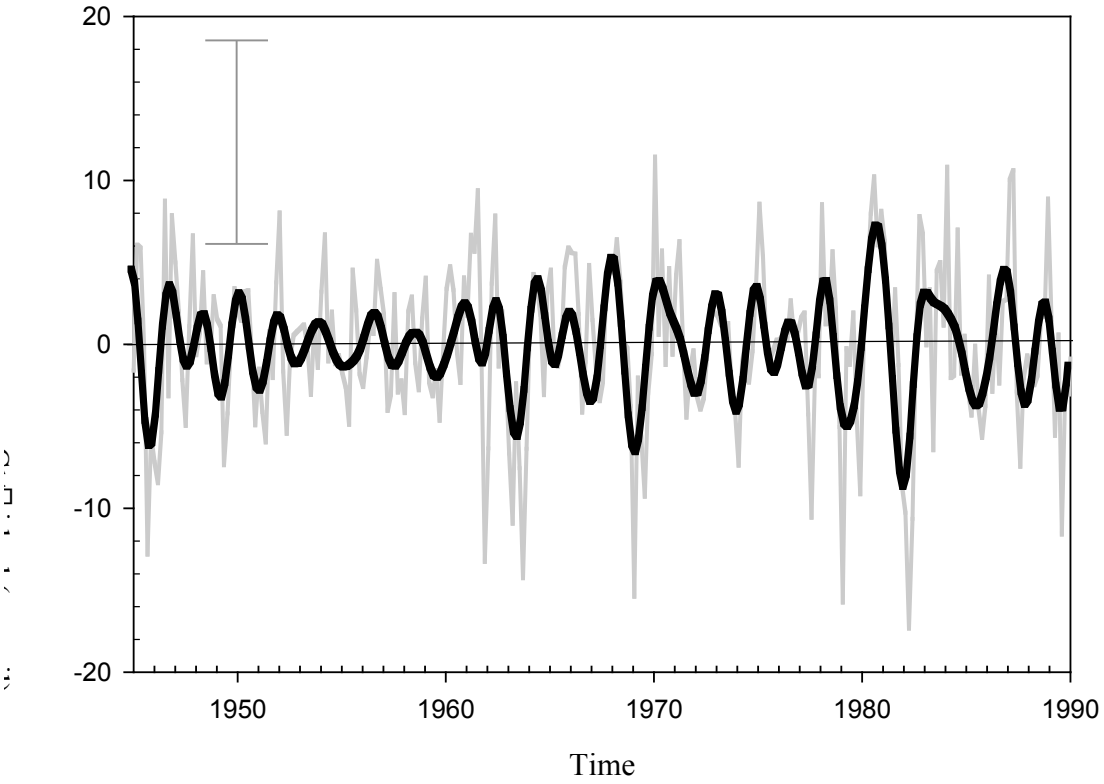

Figure 4
Time-series of bimonthly residual $\Delta^{14}C$ (per mil; normalized) for the Mentawai coral (grey line) illustrating annual to interannual variability from 1945 to 1990. Superimposed on the residual $\Delta^{14}C$ time-series is the reconstructed time-series representing the significant principal components (thick black line) at the 99% confidence interval derived from singular spectrum analysis (SSA-toolkit; Vautard et al., 1992; Dettinger et al., 1995). The reconstructed time-series exhibits interannual variability with a periodicity of 2 to 5 years.

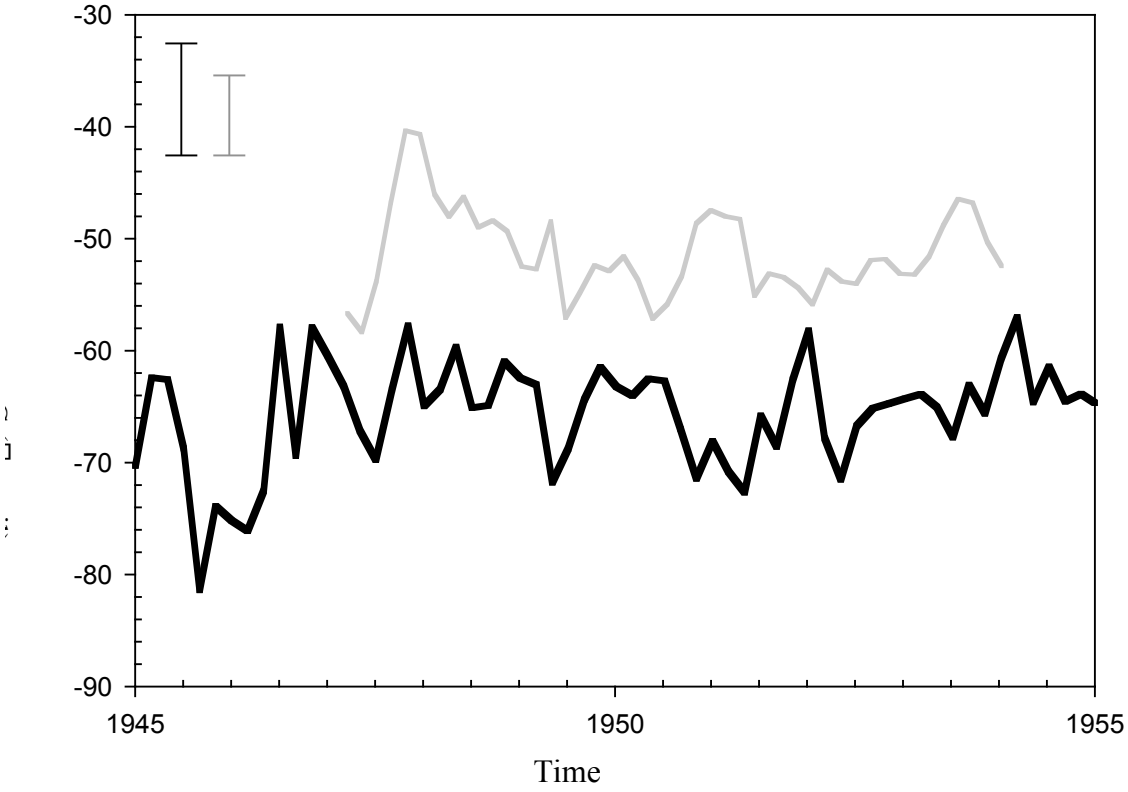

Figure 5
Time-series of pre-bomb Mentawai (black line) and Watamu (grey line) coral $\Delta^{14}C$ from 1945 to 1955. The Mentawai pre-bomb record exhibits a pre-bomb average $\Delta^{14}C$ value of -64‰, with a negligible Suess correction applied. In contrast, a 10‰ adjustment was applied to correct for the Suess effect in the Kenyan pre-bomb $\Delta^{14}C$ record, yielding a pre-bomb average of -50‰ (Grumet et al., 2002b). The steady state pre-bomb distribution across the equatorial Indian Ocean is offset by almost 15‰.

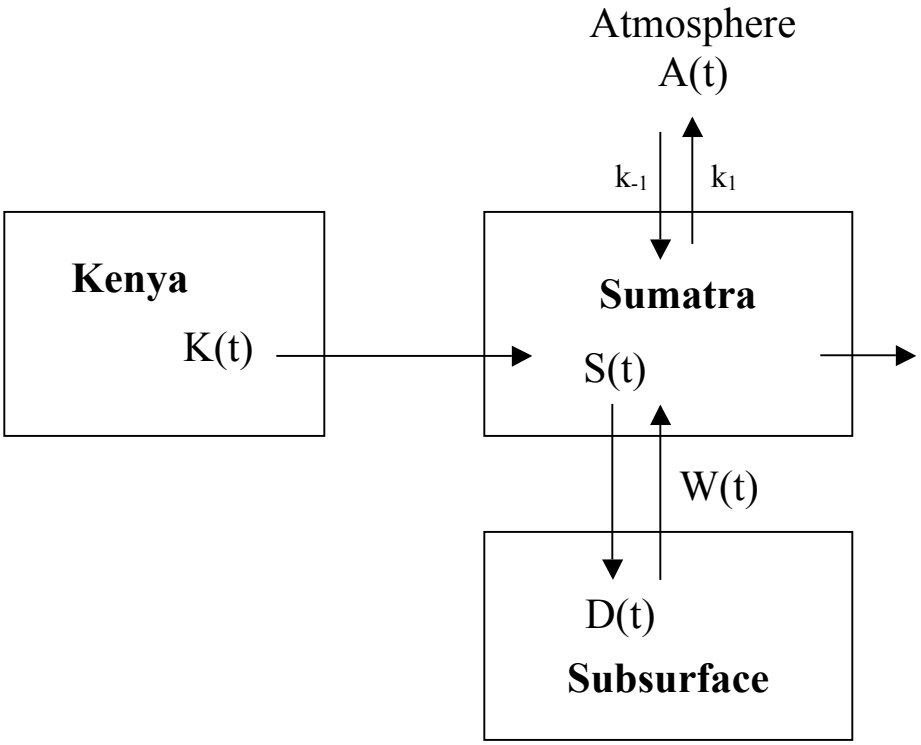

Figure 6
Schematic of the multibox model used to calculate the water mass renewal rate W(t) off the coast of Sumatra. The $\Delta^{14}C$ values at Sumatra S(t) are affected by input from Kenya surface water K(t), the atmosphere A(t) and the subsurface D(t). The fluxes of $^{14}CO_2$ into and out of the atmosphere, with respect to the ocean surface, are defined by k_1 and k_{-1}, respectively.

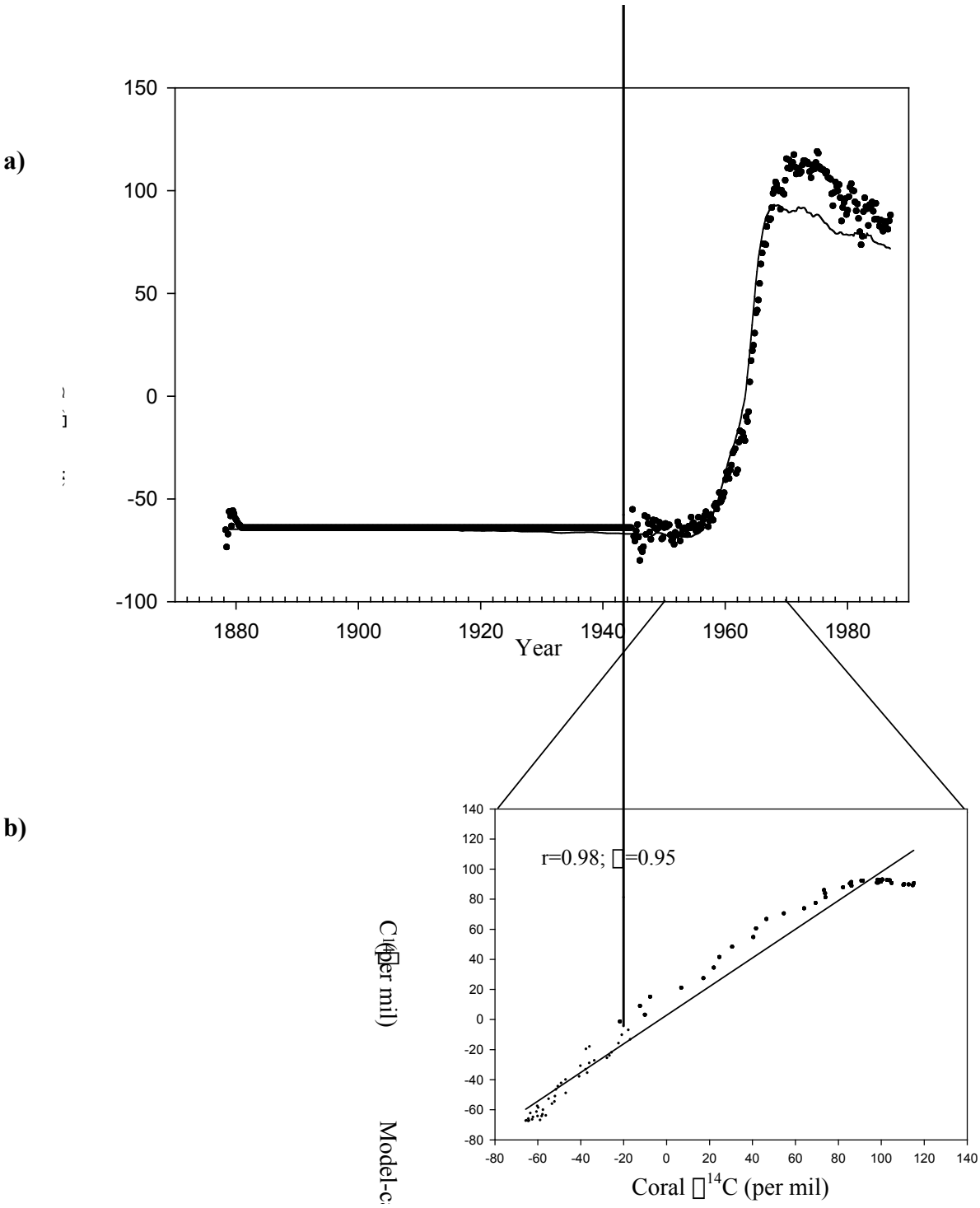

Figure 7

a) Box model results of the forward calculation (line) using a constant water mass renewal rate (W) of 0.40 yr^{-1} (2.5 yrs) to satisfy the Sumatra pre-bomb steady state $\Delta^{14}C$ value of -64‰. For comparison, the Sumatra $\Delta^{14}C$ coral time-series (dots) is superimposed on the model calculation. **b)** The Sumatra coral and model-calculated surface $\Delta^{14}C$ values are significantly correlated (r = 0.98; σ= 0.95) between 1955 and 1970 when the Watamu and Mentawai coral $\Delta^{14}C$ records diverge (Fig. 3). A constant water mass renewal rate of 0.40 yr^{-1} (~2.5 years) best explains the 2-3 year lag in the rise of Mentawai $\Delta^{14}C$ values during the initial mixing of atmospheric bomb ^{14}C.

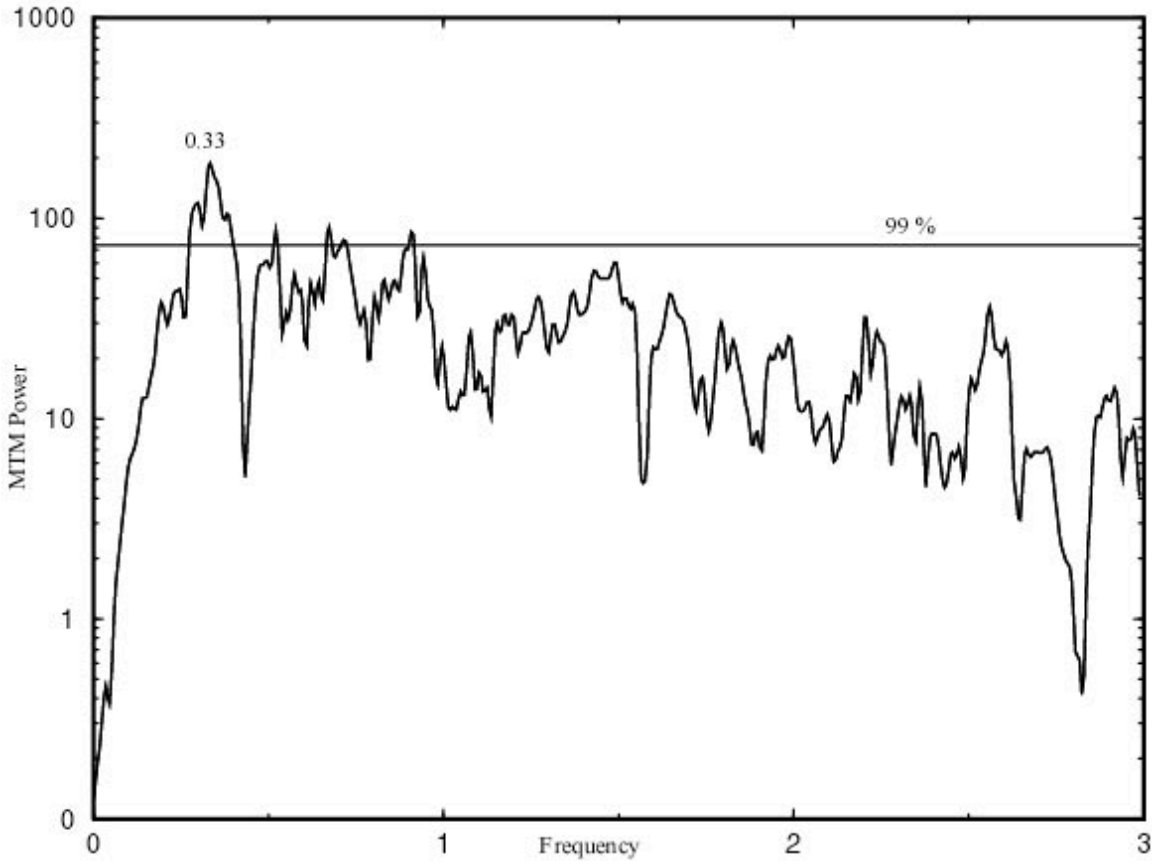

Figure 8
Spectral analysis of the detrended Mentawai coral $\Delta^{14}C$ time-series using a multi-taper method (SSA-toolkit; Vautard et al., 1992; Dettinger et al., 1995) to illustrate the significance of the 0.33 frequency (3 yr periodicity) at the 99% confidence interval.